
**Separation Science and Technology**
Publication details, including instructions for authors and subscription information:
http://www.informaworld.com/smpp/title~content=t713708471

# Resistance-in-Series for Membrane Ultrafiltration in Hollow Fibers of Tube-and-Shell Arrangement

H. M. Yeh[a]; T. W. Cheng[b]
[a] DEPARTMENT OF CHEMICAL ENGINEERING, TAMKANG UNIVERSITY, TAMSUI, TAIWAN, REPUBLIC OF CHINA [b] DEPARTMENT OF CHEMICAL ENGINEERING, NATIONAL TAIWAN UNIVERSITY, TAIPEI, TAIWAN, REPUBLIC OF CHINA

**To cite this Article** Yeh, H. M. and Cheng, T. W.(1993) 'Resistance-in-Series for Membrane Ultrafiltration in Hollow Fibers of Tube-and-Shell Arrangement', Separation Science and Technology, 28: 6, 1341 — 1355
**To link to this Article: DOI:** 10.1080/01496399308018041
**URL:** http://dx.doi.org/10.1080/01496399308018041

SEPARATION SCIENCE AND TECHNOLOGY, **28**(6), pp. 1341–1355, 1993

# Resistance-in-Series for Membrane Ultrafiltration in Hollow Fibers of Tube-and-Shell Arrangement

H. M. YEH
DEPARTMENT OF CHEMICAL ENGINEERING
TAMKANG UNIVERSITY
TAMSUI, TAIWAN, REPUBLIC OF CHINA

T. W. CHENG
DEPARTMENT OF CHEMICAL ENGINEERING
NATIONAL TAIWAN UNIVERSITY
TAIPEI, TAIWAN, REPUBLIC OF CHINA



## ABSTRACT

The effects of operating conditions on membrane ultrafiltration of dextran T500 solution in a hollow-fiber cartridge made of polysulfone have been investigated experimentally. The experimental data agree with the correlation equation based on the resistance-in-series model. It is believed that this model would also be suitable for most membrane ultrafiltration systems.

## INTRODUCTION

Ultrafiltration is a pressure-driven membrane process used for the separation of macrosolutes from a solvent, usually water. Its operational pressure is usually in the range of 10 to 100 psi. The applications of ultrafiltration included the treatment of industrial effluents, oil emulsion wastewater, biological macromolecules, colloidal paint suspensions, medical therapeutics, etc. One of the ultrafilter designs is the hollow-fiber membrane module in which the membrane is formed on the inside of tiny polymer cylinders that are then bundled and potted into a tube-and-shell arrangement. The advantages of this arrangement are low cost of investment and operation, easy flow control and cleaning, and high specific surface area per unit volume.

In membrane separation processes, solutes rejected by the membrane accumulate on the membrane surface. The concentration of solutes on the membrane surface is always higher than in the bulk solution. This is the so-called concentration polarization phenomenon. For small applied pressure, the solvent flux through the membrane is observed to be proportional to the applied pressure. As the pressure is increased further, the flux begins to drop below that which would result from linear flux–pressure behavior. Eventually a limiting flux is reached where any further pressure increase no longer results in any increase in flux. Blatt et al. (1) argued that the reason for the observed pressure independence was the formation of a gel layer on the membrane surface. Wijmans et al. (2) suggested some phenomena to account for this flux reduction: (a) a decrease of the hydraulic driving force by an osmotic pressure, (b) the resistance of the concentration polarization boundary, (c) the resistance of a gel layer, (d) an increase in membrane resistance by plugging of the pores, and (e) the resistance of an adsorption layer.



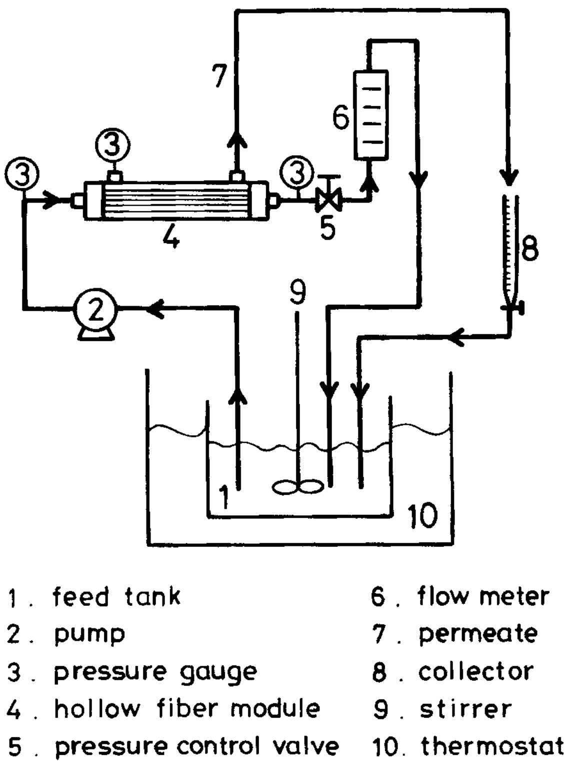


FIG. 1 Flow diagram of experimental apparatus.

The permeate flux of ultrafiltration of macromolecular solutions is usually analyzed by following models: the gel polarization model (1, 3–9), the osmotic pressure model (2, 10–17), and the resistance-in-series model (17, 18). In the gel polarization model, permeate flux is reduced by the hydraulic resistance of the gel layer, but the theoretical curves are often lower than the experimental data (3); and the concentration of the gel layer, $C_g$, was controversial, its value was not constant (7), and it did not imply the physical concentration of "gel" (17). In the osmotic pressure model, permeate flux reduction results from the decrease in effective transmembrane pressure that occurs as the osmotic pressure of the retentate increases, but it is difficult to determine the axial concentration of retentate on the surface of a hollow-fiber membrane (15, 16).

In the resistance-in-series model, permeate flux decreases due to the resistances caused by fouling or solute adsorption and concentration polarization. This method easily describes the relationships of permeate flux with operating parameters.

Chiang and Cheryan (18) analyzed the hollow-fiber ultrafiltration of skim milk by the resistance-in-series model and observed the fouling resistance was unaffected by the operating parameters as well as solute concentration. Nabetani et al. (17) measured the changes in pure water permeability of membranes caused by adsorption of solute. The experimental data showed that increasing the solute concentration increases the adsorption of solute; that is, increases the fouling resistance.

In this study we ultrafiltered macromolecular solutions in a hollow-fiber membrane module and we analyzed the permeate flux by a resistance-in-



TABLE 1
Experimental Data of Permeate Flux for Pure Water

| $u$ ($m \cdot s^{-1}$) | $\Delta P \times 10^{-5}$ Pa | $J_w \times 10^6$ $m^3 \cdot m^{-2} \cdot s^{-1}$ |
|---|---|---|
| 0.102 | 0.095 | 3.83 |
| 0.102 | 0.248 | 10.08 |
| 0.102 | 0.455 | 18.36 |
| 0.102 | 0.655 | 25.97 |
| 0.102 | 0.958 | 37.45 |
| 0.102 | 1.355 | 51.67 |
| 0.051 | 0.664 | 25.57 |
| 0.204 | 0.643 | 25.10 |
| 0.306 | 0.626 | 24.72 |

TABLE 2
Experimental Data of Permeate Flux for Dextran T500 Solution

| $C_0$ (wt%) | $u = 0.051\ m \cdot s^{-1}$ | | $u = 0.102\ m \cdot s^{-1}$ | | $u = 0.204\ m \cdot s^{-1}$ | | $u = 0.306\ m \cdot s^{-1}$ | |
|---|---|---|---|---|---|---|---|---|
| | $\Delta P \times 10^{-5}$ Pa | $J_v \times 10^6$ $m^3 \cdot m^{-2} \cdot s^{-1}$ | $\Delta P \times 10^{-5}$ Pa | $J_v \times 10^6$ $m^3 \cdot m^{-2} \cdot s^{-1}$ | $\Delta P \times 10^{-5}$ Pa | $J_v \times 10^6$ $m^3 \cdot m^{-2} \cdot s^{-1}$ | $\Delta P \times 10^{-5}$ Pa | $J_v \times 10^6$ $m^3 \cdot m^{-2} \cdot s^{-1}$ |
| 0.1 | 0.251 | 3.40 | 0.241 | 3.82 | 0.225 | 4.02 | 0.204 | 3.98 |
| | 0.451 | 4.25 | 0.443 | 4.88 | 0.426 | 5.53 | 0.406 | 5.93 |
| | 0.651 | 4.78 | 0.643 | 5.61 | 0.627 | 6.44 | 0.605 | 6.95 |
| | 0.951 | 5.37 | 0.942 | 6.24 | 0.925 | 7.27 | 0.906 | 8.17 |
| | 1.350 | 5.83 | 1.338 | 6.76 | 1.323 | 7.99 | 1.303 | 9.08 |
| 0.2 | 0.252 | 2.70 | 0.240 | 3.08 | 0.225 | 3.40 | 0.198 | 3.35 |
| | 0.452 | 3.21 | 0.442 | 3.84 | 0.424 | 4.44 | 0.400 | 4.86 |
| | 0.652 | 3.54 | 0.642 | 4.30 | 0.622 | 4.96 | 0.601 | 5.62 |
| | 0.952 | 3.82 | 0.942 | 4.67 | 0.924 | 5.52 | 0.903 | 6.36 |
| | 1.351 | 4.20 | 1.340 | 5.09 | 1.321 | 6.07 | 1.303 | 7.02 |
| 0.5 | 0.245 | 2.02 | 0.235 | 2.29 | 0.213 | 2.55 | 0.185 | 2.64 |
| | 0.446 | 2.34 | 0.433 | 2.73 | 0.413 | 3.28 | 0.388 | 3.64 |
| | 0.647 | 2.50 | 0.634 | 2.99 | 0.615 | 3.62 | 0.585 | 4.14 |
| | 0.945 | 2.67 | 0.936 | 3.21 | 0.912 | 3.98 | 0.886 | 4.57 |
| | 1.339 | 2.86 | 1.340 | 3.46 | 1.317 | 4.28 | 1.287 | 5.00 |
| 1.0 | 0.243 | 1.54 | 0.228 | 1.73 | 0.200 | 1.92 | 0.165 | 1.85 |
| | 0.445 | 1.79 | 0.429 | 2.07 | 0.400 | 2.50 | 0.365 | 2.64 |
| | 0.642 | 1.93 | 0.629 | 2.29 | 0.600 | 2.78 | 0.564 | 3.03 |
| | 0.942 | 2.06 | 0.930 | 2.46 | 0.901 | 3.05 | 0.864 | 3.36 |
| | 1.337 | 2.18 | 1.330 | 2.62 | 1.299 | 3.24 | 1.264 | 3.62 |
| 2.0 | 0.236 | 1.09 | 0.211 | 1.21 | 0.165 | 1.26 | 0.216 | 1.60 |
| | 0.435 | 1.30 | 0.410 | 1.52 | 0.363 | 1.81 | 0.316 | 1.94 |
| | 0.635 | 1.43 | 0.611 | 1.69 | 0.563 | 2.06 | 0.513 | 2.34 |
| | 0.935 | 1.56 | 0.911 | 1.84 | 0.862 | 2.29 | 0.813 | 2.68 |
| | 1.327 | 1.66 | 1.311 | 1.96 | 1.260 | 2.49 | 1.214 | 2.92 |

series model. The effects of operating conditions on the resistances and the correlation equations for the resistances were developed. These correlation equations show that the resistances are functions of operating parameters such as the transmembrane pressure, the solute concentration, and the flow velocity.

## RESISTANCE-IN-SERIES MODEL

The resistance-in-series approach will be employed in this research to model the permeate flux. In this model, permeate flux $J_v$ may be expressed as

$$J_v = \frac{\Delta P}{R_m + R_f + R_p} \tag{1}$$

where $R_m$ denotes the intrinsic resistance of a membrane, and $R_p$ and $R_f$ are, respectively, the resistances due to the concentration polarization/gel



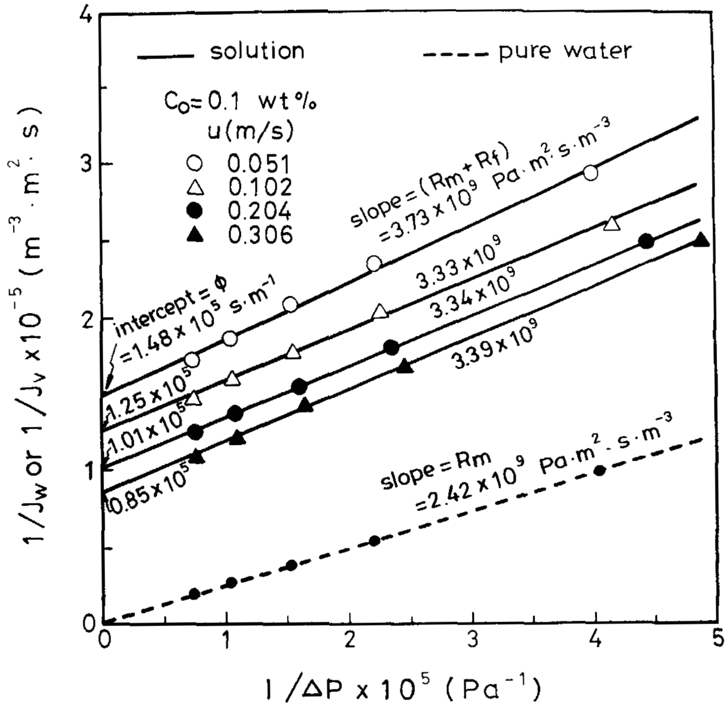


FIG. 2 Relations between $1/J_v$ and $1/\Delta P$, and between $1/J_w$ and $1/\Delta P$.

layer and those due to other fouling phenomena such as solute adsorption, while $\Delta P$ is the transmembrane pressure defined as

$$\Delta P = \frac{P_i + P_o}{2} - P_p \quad (2)$$

In Eq. (2), $P_i$ and $P_o$ are, respectively, the inlet and outlet pressures of the tubeside and $P_p$ is the permeate pressures of the shellside.

When pure water is ultrafiltrated with a fresh hollow-fiber module, neither $R_f$ nor $R_p$ exists and Eq. (1) reduces to

$$J_w = \Delta P/R_m \quad (3)$$



TABLE 3
The Fitting Parameters of Experimental Data[a]

| $C_0$ (wt%) | $u$ ($m \cdot s^{-1}$) | $(R_m + R_f) \times 10^{-9}$ $Pa \cdot m^2 \cdot s \cdot m^{-3}$ | $R_f \times 10^{-9}$ $Pa \cdot m^2 \cdot s \cdot m^{-3}$ | $\phi \times 10^{-5}$ $s \cdot m^{-1}$ |
|---|---|---|---|---|
| 0.1 | 0.051 | 3.73 | 1.31 | 1.48 |
| | 0.102 | 3.33 | 0.91 | 1.25 |
| | 0.204 | 3.34 | 0.92 | 1.01 |
| | 0.306 | 3.39 | 0.97 | 0.85 |
| 0.2 | 0.051 | 3.95 | 1.53 | 2.17 |
| | 0.102 | 3.66 | 1.24 | 1.74 |
| | 0.204 | 3.42 | 1.00 | 1.43 |
| | 0.306 | 3.61 | 1.19 | 1.16 |
| 0.5 | 0.051 | 4.16 | 1.74 | 3.28 |
| | 0.102 | 4.06 | 1.64 | 2.66 |
| | 0.204 | 3.93 | 1.51 | 2.08 |
| | 0.306 | 3.81 | 1.39 | 1.74 |
| 1.0 | 0.051 | 5.51 | 3.09 | 4.24 |
| | 0.102 | 5.25 | 2.83 | 3.50 |
| | 0.204 | 4.92 | 2.50 | 2.74 |
| | 0.306 | 4.94 | 2.52 | 2.40 |
| 2.0 | 0.051 | 8.93 | 6.51 | 5.46 |
| | 0.102 | 7.75 | 5.33 | 4.58 |
| | 0.204 | 7.31 | 4.89 | 3.49 |
| | 0.306 | 7.38 | 4.96 | 2.82 |

[a] $R_m = 2.42 \times 10^9$ $Pa \cdot m^2 \cdot s \cdot m^{-3}$.

Therefore, the intrinsic resistance of a membrane is the slope of the following straight line with $1/J_v$ as the ordinate and $1/\Delta P$ as the abscissa.

$$\frac{1}{J_w} = R_m\left(\frac{1}{\Delta P}\right) \tag{3'}$$

$R_p$ will be proportional to the amount and the specific hydraulic resistance of the deposited layer. Since the deposited layer is compressible, $R_p$ is a function of pressure, so that

$$R_p = \phi \Delta P \tag{4}$$

Accordingly, Eq. (1) may be rewritten as

$$J_v = \frac{\Delta P}{R_m + R_f + \phi \Delta P} \tag{5}$$

in which $R_m$, $R_f$, and $\phi$ will be determined by experimental data.



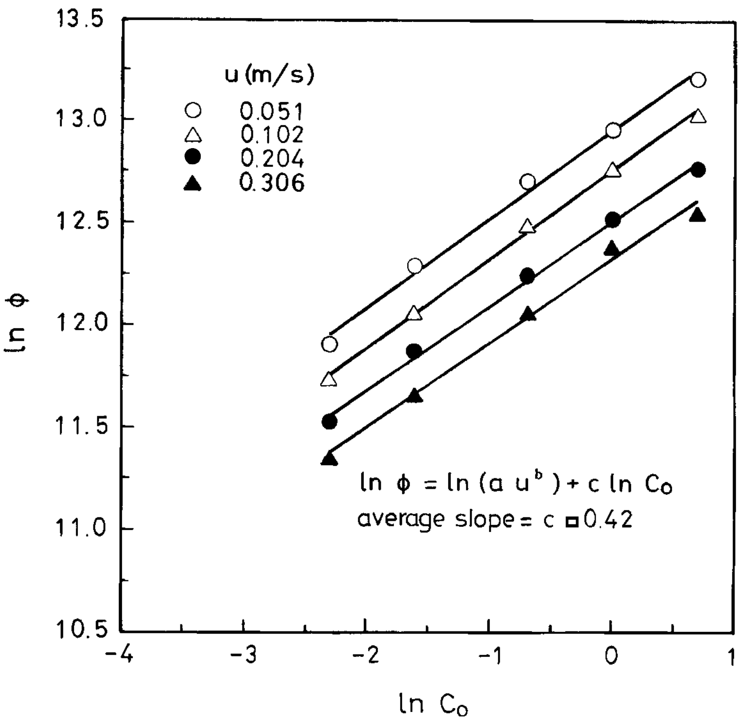


FIG. 3 Relation between $\phi$ and $C_0$.

It is noted from Eq. (5) that when $\Delta P$ is low, $J_v$ is primarily controlled by $(R_m + R_f)$. However, when $\Delta P$ is large, $J_v$ would approach the value of $1/\phi$.

## EXPERIMENTAL METHOD

### Apparatus and Materials

The flow sheet of an ultrafiltration apparatus is shown in Fig. 1. An Amicon model H1P30-20 hollow-fiber cartridge (Amicon Corp., Danvers, Massachusetts) was used. The fiber (i.d. 0.05 cm, effective length 15.3 cm) was made of polysulfone and the total effective membrane area was 600 $cm^2$.

The tested solute was dextran T500 (Pharmacia, $M_n$ = 170,300 and $M_w$ = 503,000). It was more than 99% retained by the membrane used. The solvent was ion exchange pure water.

The feed solution was circulated by a high-pressure pump with a variable speed moter (L-07553-20, Cole-Parmer Co., Chicago, Illinois), and the



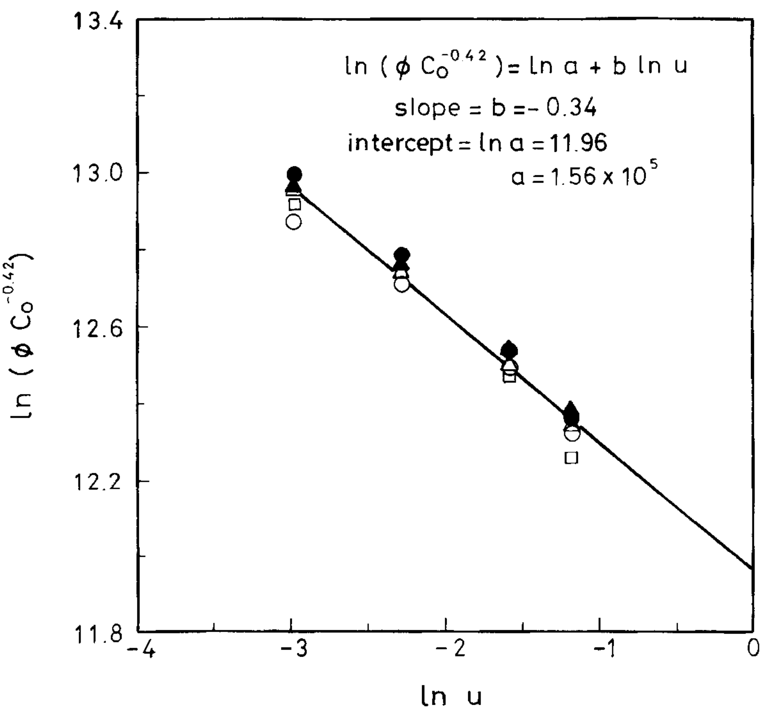


FIG. 4 Relation between $\phi C_0^{-0.42}$ and $u$.

feed flow was measured with a flowmeter (L-03217-34, Cole-Parmer Co.). The pressure was measured with a pressure transmitter (Model 891.14.425, Wika).

## Experimental Conditions and Procedure

The experimental conditions were as follows. The feed solution concentrations were 0.1, 0.2, 0.5, 1.0, and 2.0 wt% dextran T500; the feed flow velocities were 0.051, 0.102, 0.204, and 0.306 m/s; and the feed inlet pressures were 30, 50, 70, 100, and 140 kPa. The feed solution temperature in all experiments was kept at 25°C by a thermostat. During a run, both permeate and retentate were recycled back to the feed tank to keep the feed concentration constant.

The experimental procedure was as follows. First, a fresh hollow-fiber module was used to determine the intrinsic resistance of membrane $R_m$. Permeate fluxes for pure water $J_w$ were measured under various transmembrane pressures and flow velocities. Then the feedwater was replaced



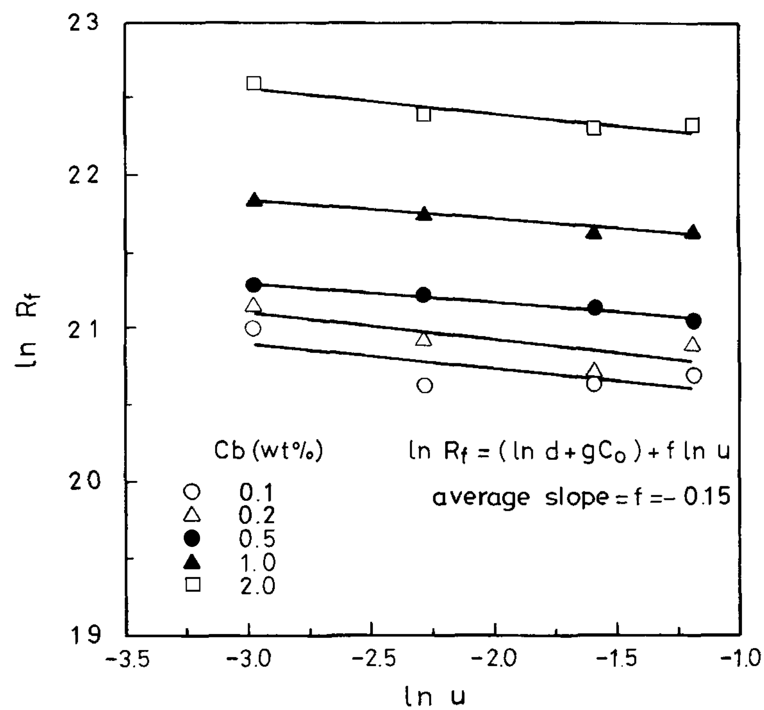


FIG. 5 Relation between $R_f$ and $u$.

with the tested solution. Permeate fluxes for dextran T500 solution $J_v$ were measured under all operating conditions at steady state. Values of permeate flux reached steady state within 30 to 120 minutes.

After each solution run, the membrane module was cleaned by a combination of high circulation and backflushing with pure water. The cleaning procedure was repeated until the original water flux had been restored.

## RESULTS AND DISCUSSION

The experimental data of the permeate flux for pure water, $J_w$, are presented in Table 1 while that of solution permeate flux, $J_v$, are given in Table 2.

### Determination of $R_m$

The intrinsic resistance of the hollow-fiber membrane module employed in this study was determined by Eq. (3) coupled with the use of Table 1.



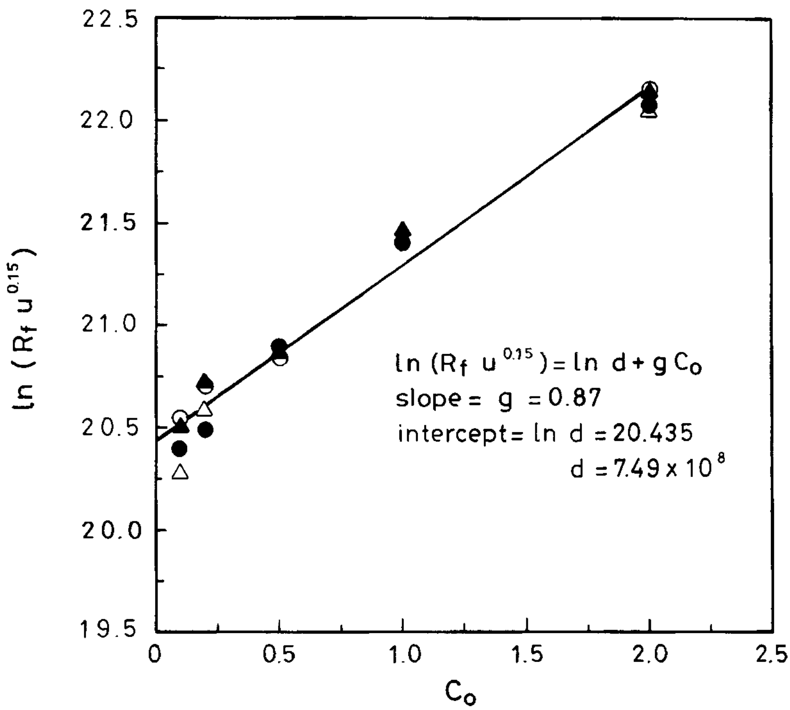


FIG. 6 Relation between $R_f u^{0.15}$ and $C_0$.

It is shown in Fig. 2 that under various transmembrane pressures and flow velocities of water the measured value of the intrinsic resistance for the membrane system used in present study is

$$R_m = 2.42 \times 10^9 \ \text{Pa}\cdot\text{m}^2\cdot\text{s}\cdot\text{m}^{-3} \tag{6}$$

## Determination of $R_f$ and $\phi$

It was found from experimental data that at a certain flow velocity $u$ and feed concentration $C_0$ a straight line of $1/J_v$ vs $1/\Delta P$ can be constructed by the least-squares method. This means that Eq. (5) correlates the experimental data quite well, for it can be rewritten as

$$\frac{1}{J_v} = \phi + \frac{(R_m + R_f)}{\Delta P} \tag{7}$$

in which both the intersection at ordinate $\phi$ and the slope $(R_m + R_f)$ of this straight line are functions of $u$ and $C_0$. Figure 2 illustrates the method



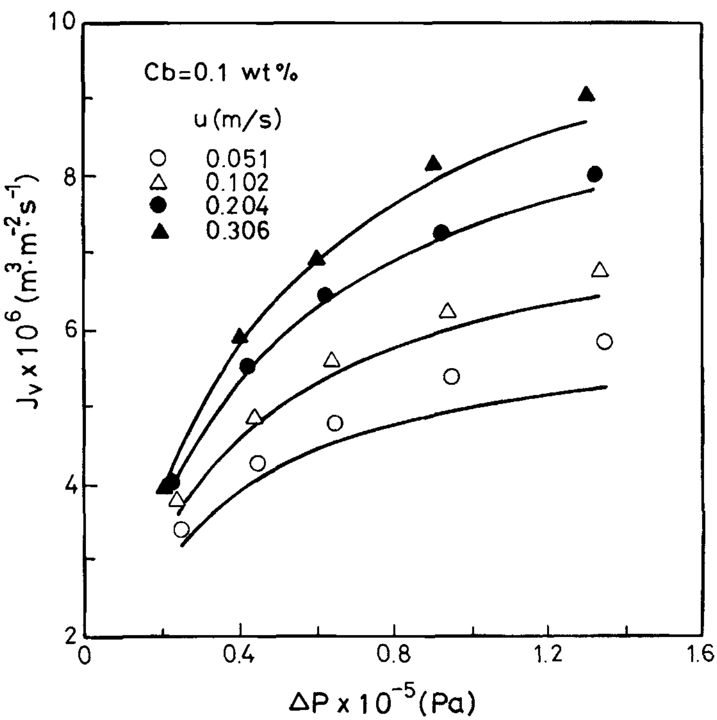


FIG. 7 Relation between $J_v$ and $\Delta P$ for $C_0 = 0.1$ wt%.

for determining $\phi$ and $(R_m + R_f)$ for $C_0 = 0.1$ wt%; all the values determined are listed in Table 3. It is noted that $R_f$ is determined by

$$R_f = (R_m + R_f) - 2.42 \times 10^9 \text{ Pa·m}^2\text{·s·m}^{-3} \quad (8)$$

## Correlation Equation for $\phi$

Since $\phi$ is a function of the flow velocity and feed concentration, we let

$$\phi = au^bC_0^c \quad (9)$$

in which $a$, $b$, and $c$ are constants. Accordingly, values of $a$, $b$, and $c$ were determined in Figs. 3 and 4 with the use of Table 3. The correlation equation for $\phi$ thus obtained is

$$\phi = 1.56 \times 10^5\, u^{-0.34}C_0^{0.42} \text{ s·m}^{-1} \quad (10)$$

## Correlation Equation for $R_f$

$R_f$ is also a function of $u$ and $C_0$, but we assume that

$$R_f = du^f \exp(gC_0) \quad (11)$$

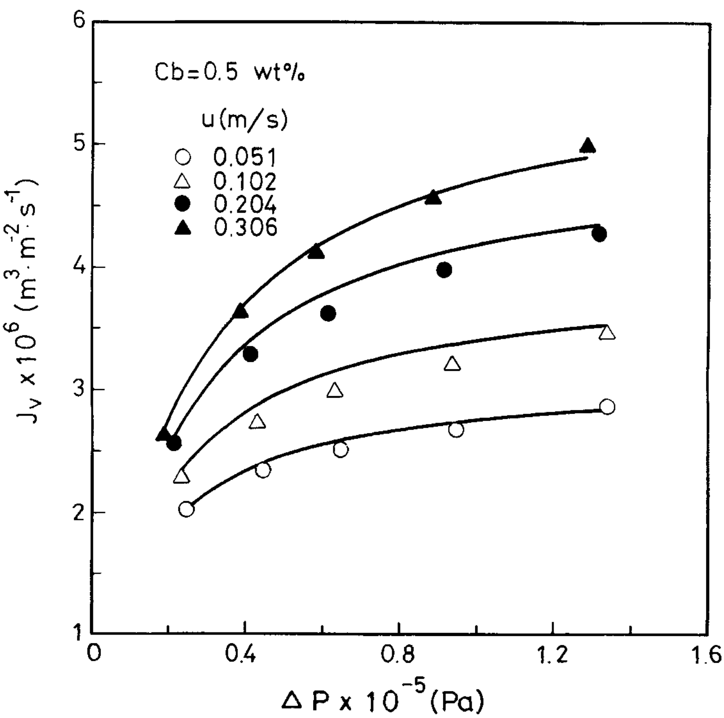


FIG. 8 Relation between $J_v$ and $\Delta P$ for $C_0 = 0.5$ wt%.

in which $d$, $f$, and $g$ are constants. Values of $d$, $f$, and $g$ were determined in Figs. 5 and 6 with the use of Table 3. The correlation equation for $R_f$ is

$$R_f = 7.49 \times 10^8 u^{-0.15} \exp(0.87C_0) \quad \text{Pa·m}^2\text{·s·m}^{-3} \tag{12}$$

### Correlation Equation for $J_v$

Substitution of Eqs. (6), (10), and (12) into Eq. (5) obtained the complete correlation equation for permeate flux as

$$J_v = \frac{\Delta P}{2.42 \times 10^9 + 7.49 \times 10^8 u^{-0.15} e^{0.87C_0} + 1.56 \times 10^5 u^{-0.34} C_0^{0.42} \Delta P} \tag{13}$$

Both the permeate fluxes calculated from Eq. (13) and these obtained from the experiment for $C_0$ = 0.1, 0.5, and 2.0 wt% dextran T500 are shown in Figs. 7, 8, and 9 for comparison. It is seen from these figures that Eq. (13) correlates the experimental data pretty well.



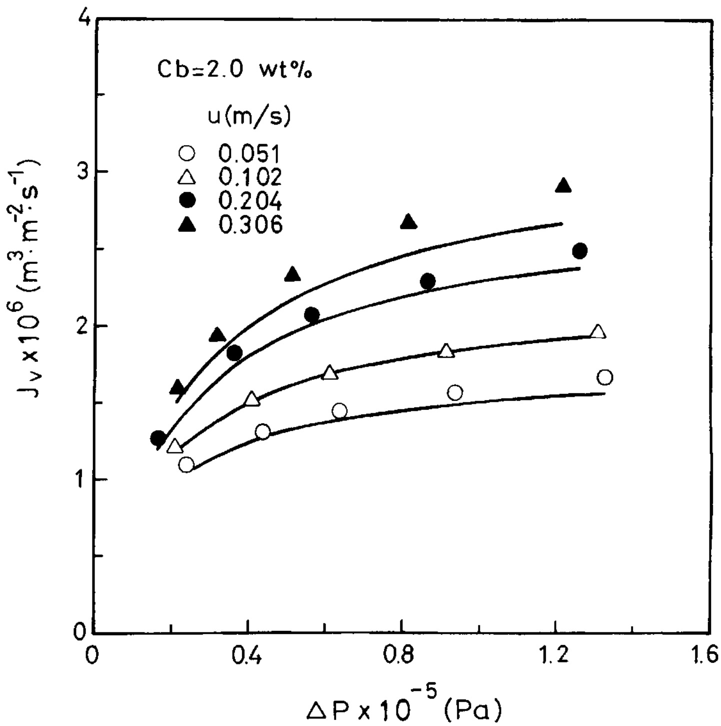


FIG. 9 Relation between $J_v$ and $\Delta P$ for $C_0$ = 2.0 wt%.

## CONCLUSIONS

The effects of transmembrane pressure $\Delta P$, flow velocity $u$, and feed concentration $C_0$ on permeate flux $J_v$ in membrane ultrafiltration have been investigated experimentally. As expected, it is seen from the experimental results (Table 2 or Figs. 7, 8, and 9) that $J_v$ increases as $\Delta P$ or $u$ increases, but decreases when $C_0$ increases. We also found in this study that Eq. (5), as well as the resistance-in-series model, successfully correlate the experimental results obtained for the ultrafiltration of dextran T500 solution in an Amicon model H1P 30-20 hollow-fiber cartridge made of polysulfone under the present experimental conditions. Since the resistance-in-series model easily describes the relationships of permeated flux with operating parameters, we believe that this model will also be suitable for most membrane ultrafiltration systems including systems with different kinds of feed solutions, different materials of hollow fiber, and various design and operating conditions.



## SYMBOLS

| | |
|---|---|
| $a$, $b$, $c$ | constant defined by Eq. (9) |
| $C_0$ | concentration of feed solution (wt% dextran T500) |
| $d$, $f$, $g$ | constant defined by Eq. (11) |
| $J_v$ | volume permeate flux of solution ($m^3 \cdot m^{-2} \cdot s^{-1}$) |
| $J_w$ | volume permeate flux of pure water ($m^3 \cdot m^{-2} \cdot s^{-1}$) |
| $P_i$, $P_o$ | inlet, outlet pressure of the tubeside (Pa) |
| $P_p$ | permeate pressure of the shellside (Pa) |
| $\Delta P$ | transmembrane pressure defined by Eq. (2) (Pa) |
| $R_f$ | resistance due to solute adsorption and fouling ($Pa \cdot m^2 \cdot s \cdot m^{-3}$) |
| $R_m$ | intrinsic resistance of membrane ($Pa \cdot m^2 \cdot s \cdot m^{-3}$) |
| $R_p$ | resistance due to concentration polarization/gel layer ($Pa \cdot m^2 \cdot s \cdot m^{-3}$) |
| $u$ | feed flow velocity ($m \cdot s^{-1}$) |
| $\phi$ | parameter of concentration polarization defined by Eq. (4) ($s \cdot m^{-1}$) |

## ACKNOWLEDGMENT

The authors wish to express their thanks to the Chinese National Science Council for financial aid.

## REFERENCES

1. W. F. Blatt, A. Dravid, A. S. Michaels, and L. Nelsen, in *Membrane Science and Technology*, Plenum Press, New York, 1970, pp. 47–97.
2. J. G. Wijmans, S. Nakao, and C. A. Smolders, *J. Membr. Sci.*, *20*, 115 (1984).
3. M. C. Porter, *Ind. Eng. Chem.*, *Prod. Res. Dev.*, *11*, 234 (1972).
4. R. B. Grieves, D. Bhattacharyya, W. G. Schomp, and J. L. Bewley, *AIChE J.*, *19*, 766 (1973).
5. J. J. S. Shen and R. F. Probstein, *Ind. Eng. Chem.*, *Fundam.*, *16*, 459 (1977).
6. R. F. Probstein, W. Leung, and Y. Alliance, *J. Phy. Chem.*, *83*, 1228 (1979).
7. S. Nakao, T. Nomura, and S. Kimura, *AIChE J.*, *25*, 615 (1979).
8. A. G. Fane, C. J. D. Fell, and A. G. Waters, *J. Membr. Sci.*, *9*, 245 (1981).
9. A. G. Fane, *Ibid.*, *20*, 249 (1984).
10. A. A. Kozinski and E. N. Lightfoot, *AIChE J.*, *18*, 1030 (1972).
11. W. Leung and R. F. Probstein, *Ind. Eng. Chem.*, *Fundam.*, *18*, 274 (1979).
12. R. P. Wendt, E. Klein, F. F. Holland, and K. E. Eberle, *Chem. Eng. Commun.*, *8*, 251 (1981).
13. S. Nakao and S. Kimura, *J. Chem. Eng. Jpn.*, *15*, 200 (1982).
14. C. Kleinstreuer and M. S. Paller, *AIChE J.*, *29*, 529 (1983).
15. M. J. Clifton, N. Abidine, P. Aptel, and V. Sanchez, *J. Membr. Sci.*, *21*, 233 (1984).
16. R. P. Ma, C. H. Gooding, and W. K. Alexander, *AIChE J.*, *31*, 1728 (1985).
17. H. Nabetani, M. Nakajima, A. Watanabe, S. Nakao, and S. Kimura, *Ibid.*, *36*, 907 (1990).
18. B. H. Chiang and M. Cheryan, *J. Food Sci.*, *51*, 340 (1986).

*Received by editor May 12, 1992*